Applied Catalysis B: Environmental 176–177 (2015) 70–75

Contents lists available at ScienceDirect

Applied Catalysis B: Environmental

journal homepage: www.elsevier.com/locate/apcatb

Antimicrobial properties of highly efficient photocatalytic TiO_2 nanotubes

Joanna Podporska-Carroll[a], Eugen Panaitescu[b], Brid Quilty[c], Lili Wang[b], Latika Menon[b,**], Suresh C. Pillai[d,e,*]

[a] Centre for Research in Engineering Surface Technology (CREST), FOCAS Institute, Dublin Institute of Technology, Kevin Street, Dublin 8, Ireland
[b] Department of Physics, Northeastern University, Boston, MA 02115, USA
[c] School of Biotechnology, Dublin City University, Dublin 9, Ireland
[d] Centre for Precision Engineering, Materials and Manufacturing Research (PEM), Institute of Technology Sligo, Ash Lane, Sligo, Ireland
[e] Nanotechnology Research Group, Department of Environmental Science, School of Science, Institute of Technology Sligo, Ash Lane, Sligo, Ireland

ARTICLE INFO

Article history:
Received 8 December 2014
Received in revised form 6 March 2015
Accepted 19 March 2015
Available online 20 March 2015

Keywords:
Photocatalysis
Nanotube
Antibacterial
Hydroxyl radical
Amorphous
Partially crystalline
E. coli and *S. aureus*
Evonic-Degussa P25
Advanced oxidation process (AOP)

ABSTRACT

A rapid chlorine-based electrochemical anodization method resulted in the production of free-standing bundles of titania (TiO_2) nanotubes with high-aspect ratio (up to 100 μm long and about 20 nm in diameter). XRD and Raman spectroscopy revealed the presence of partially crystalline amorphous titania nanostructures modified with surface hydroxyl groups. Photocatalytic antimicrobial properties of these nanotubes have been investigated using *Escherichia coli* and *Staphylococcus aureus* and compared with a commercial reference sample, Evonic-Degussa P25. Titania nanotubes were found to be highly efficient in inactivating both *E. coli* (97.53%) and *S. aureus* (99.94%) in under 24 h of UV irradiation. On the other hand, commercial Evonik Degussa P-25 titania nanoparticles and control samples did not reveal antimicrobial properties for the same amount of time under either light or dark conditions. These results indicate that along with material properties, the high-aspect ratio nanotube architecture, surface hydroxyls, physico-chemical properties of TiO_2 nanotubes as well as experimental conditions of the biological investigations play a significant role in the antibacterial activity.

1. Introduction

Titanium dioxide is an extensively studied semiconductor due to its great potential in the photocatalytic degradation of organic pollutants and bacteria [1–6]. Recently, there has been a great influx of interest in using nanostructured titania for enhancing the efficiency of photocatalytic applications. In this regard, the nanotube architecture is one of the most promising morphologies for antimicrobial applications because of desirable features such as high-aspect ratio, enhanced active surface area and improved light harvesting and trapping. While titania nanotubes have been produced in the past either using a hydrothermal method or using a fluoride-based electrochemical method, a novel and efficient route for the synthesis of very long, high-aspect ratio nanotubes (up to 100 μm long and about 20 nm in diameter) using a simple chlorine-based electrochemical method has been recently demonstrated [7–9]. This procedure results in the production of free-standing bundles of nanotubes with surface hydroxyl groups. Such high-aspect ratio, surface hydroxyl rich and highly porous particles can be directly used for photocatalytic antimicrobial applications.

The photocatalytic process involves the formation of electron (e^-_{CB}) and hole (h^+_{VB}) pairs upon the irradiation of light that exceeds the band gap energy (3.2 eV) of TiO_2. Positive holes (h^+_{VB}) become trapped by water molecules in the atmosphere. The water molecule is oxidized by h^+_{VB} producing H^+ and •OH radicals, which are extremely powerful oxidants [1,2]. The hydroxyl radicals then oxidize organic molecules from the surrounding environment to final products such as CO_2, mineral acids and H_2O. Electrons in the conduction band (e^-_{CB}) can be rapidly trapped by atmospheric

* Corresponding author.
** Corresponding author at: Nanotechnology Research Group, Department of Environmental Science, School of Science, Institute of Technology Sligo, Ash Lane, Sligo, Ireland. Tel.: +353 719305816.
E-mail addresses: l.menon@neu.edu (L. Menon), Pillai.Suresh@itsligo.ie (S.C. Pillai).

http://dx.doi.org/10.1016/j.apcatb.2015.03.029
0926-3373/

oxygen. The oxygen can further be reduced by e^-_{CB} to form superoxide ($O^{2-\bullet}$) radicals that will further combine with H^+, to form peroxide radicals ($^\bullet OOH$) and hydrogen peroxide, H_2O_2. These reactive oxidation species produced during the irradiation process are able to oxidize the majority of volatile organic compounds (VOC) and organic matters such as bacteria until complete mineralization . The objective of the current investigation was to understand the antimicrobial properties of the hydroxyl group modified titania nanotubes which are produced by rapid breakdown anodization.

2. Experimental

2.1. Synthesis and characterization of titania nanotube powders

Powders of amorphous titanium dioxide (titania) nanotubes have been synthesized by DC (V = 16 V) rapid breakdown anodization [7–9] of 0.89 mm thick titanium foil (Alfa Aesar, 99.7% metal basis) for several hours in an aqueous solution containing 0.1 M ammonium chloride (Alfa Aesar, purity >99.5%). Bundles of nanotubes were continuously released in the solution from corrosion sites on the titanium foil surface, forming a white precipitate which was recovered, washed repeatedly with water and then with isopropanol, and subsequently dried on a hotplate at about 80 °C. BET (Porous Materials, Inc.) measurements were performed on approximately 0.5 g of powder which was degassed to 20 mTorr at 20 °C prior to measurements, with nitrogen at −195.76 °C used as adsorbate. Separately, bundles of nanotubes were released on a conductive substrate or directly on a transmission electron microscopy (TEM) grid for further examination by scanning electron microscopy (SEM) (Hitachi S4800) or TEM (JEOL 2010F). In addition, the powders were further analysed by Raman spectroscopy (Jobin Yvon LabRam HR800) and X-ray Diffraction (XRD) (PANalytical X'Pert Pro Philips).

2.2. Determination of antimicrobial activity

2.2.1. Preparation of organisms

Gram-negative *Escherichia coli* (ATCC 25922) and gram-positive *Staphylococcus aureus* (ATCC 6538) were chosen to conduct a pure culture study in suspension. First, sterile aliquots of nutrient broth (Oxoid) and Columbia broth (Difco) were inoculated with *E. coli* and *S. aureus*,respectively, and incubated overnight at 37 °C. Next, they were centrifuged, washed with phosphate buffered saline (PBS) and their concentration was adjusted accordingly.

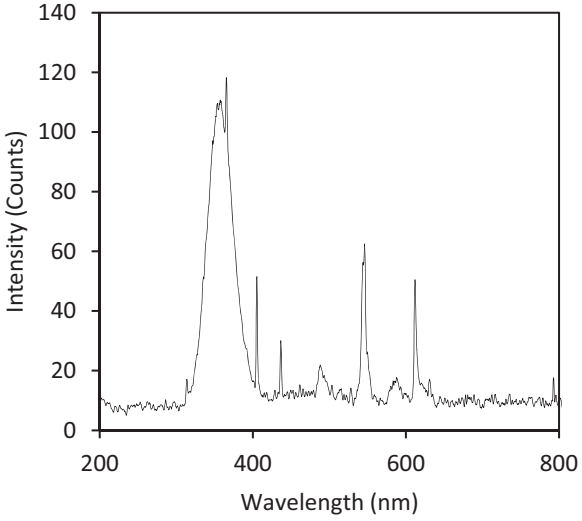

Fig. 1. Emission spectrum of the UV-A/B lamp – light source used in the experiment.

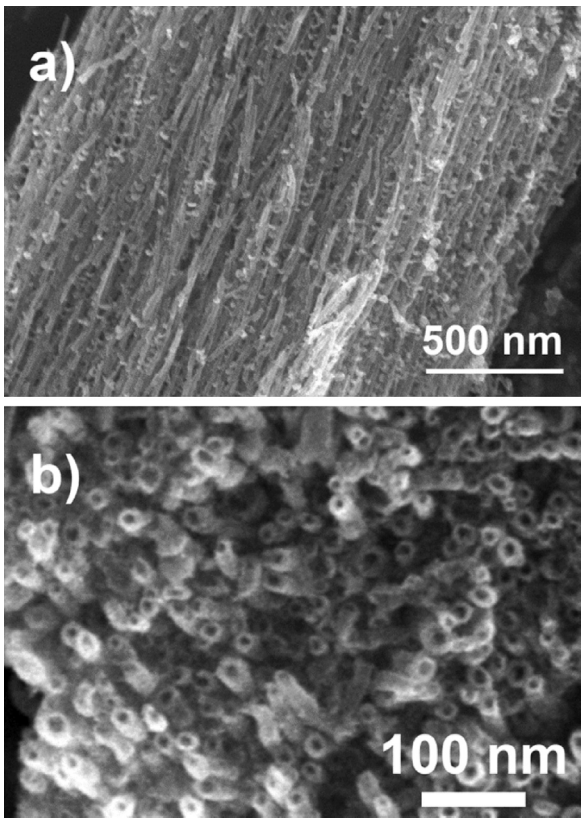

Fig. 2. SEM images of titania nanotubes-based powders; (a) side view of a microscopic grain which is in fact a compact bundle of ordered titania nanotubes; (b) top view of another grain clearly showing tightly bound nanotubes with a diameter of about 20 nm.

2.2.2. Microbiological evaluation

In order to evaluate an effect of TiO_2 nanotubes (TiO_2-NT) on the selected microorganisms, 50 mg/mL suspensions of nano-powders in Müeller-Hinton (M-H) broth were prepared. The effect of TiO_2 nanotubes on activity of *E. coli* and *S. aureus* was determined by evaluation of growth of the cultures in the presence of nano-photocatalyst compared with the growth of the culture in medium only. Commercially available photocatalyst Evonik-Degussa P25 (P25) of the same concentration served as a reference material. Sterile M-H broth or the same broth inoculated with bacteria only served as negative and positive controls, respectively. All solutions were prepared using aseptic methods. For testing, wells of sterile polystyrene plates were filled with 5 mL of previously prepared solutions. Next, bacterial suspensions were added and the final concentration in each well was adjusted to approximately 10^4 colony-forming units/mL (CFU/mL). The prepared systems were divided into two groups: one was exposed to the source of UV-AB light with the emission spectrum presented in Fig. 1, and another left without light access for a total period of 24 h. Samples from both groups were taken at 0, 1, 6 and 24 h of the experiment for further evaluation. The pour plate technique was used to determine the number of surviving organisms. For the microbiological evaluation, samples were tested in triplicate. The results were presented as the mean ± standard deviation.

3. Results and discussion

SEM imaging (Fig. 2) revealed that each microscopic powder grain is in fact a bundle of highly ordered ultra-high aspect ratio titania nanotubes, with average outer diameters around 20 nm and lengths of the order of tens of microns. The grain size is widely

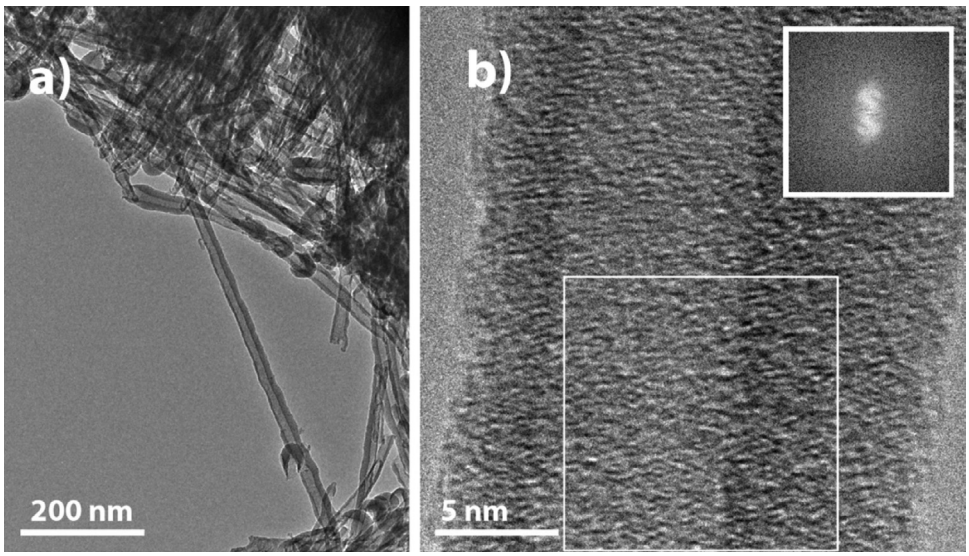

Fig. 3. Characterization of titania nanotubes powders. (a) Low magnification TEM image of a bundle of nanotubes (b) HRTEM of a single nanotube; inset is showing the Fast Fourier Transform of the region marked by a white square.

distributed from sub-micron all the way to several tens of microns, usually the grains having an elongated shape in the direction parallel to the nanotubes that are forming them. As reported in a previous work [9], the nanotubes are tightly packed within the bundles with a density of about 800 tubes/μm^2, corresponding to an estimated active surface area of 108 $\mu m^2/\mu m^3$. Further BET measurements indicated a surface area of about 150 m^2/g with a total pore volume of 0.283 cm^3/g, which corresponds to an average (inner) pore diameter of approximately 8 nm.

TEM imaging (Fig. 3) confirmed tubular morphology, with a tube diameter of about 20 nm and wall thickness around 5 nm. Moreover, on the HRTEM image no ordering was observed over long ranges, as confirmed also by the Fast Fourier Transform analysis. Thus, the tubes are mostly amorphous with possible local weak crystallization areas. Indeed, as synthesized, the nanotubes are amorphous and all powders used throughout this work were used as is. However, if needed, crystallization could be achieved by annealing the powders at temperatures above 300 °C [7–9]. XRD (Fig. 4a) and Raman (Fig. 4b and c) measurements confirmed that the nanotubes were mostly amorphous. The XRD spectrum, typical for partially crystalline with amorphous titania nanostructures [10], exhibits only a very broad maximum around the main theoretical anatase peak ($2\theta = 25.3°$). Previous XPS studies on the material [11] confirmed that the chemical bonds between Ti and O correspond to the TiO_2 molecule. Indeed, the Ti peaks were assigned to Ti^{4+} in a tetragonal structure, and the O peak to the Ti—O bond in TiO_2. On the other hand the Ti:O ratio is not at the stoichiometric value of 1:2, the amorphous as synthesized nanotubes being deficient in oxygen.

Raman spectroscopy has been performed in order to ascertain both the crystallinity of titania, and the presence of hydroxyl groups on the surface of the nanotubes. Because Ti, O, and H have large atomic mass differences, we assumed that the observed phonons are almost pure modes, corresponding to displacements of single atomic species, with the generally accepted rule of thumb that large wavenumbers correspond to displacements of light ions [12]. For low wavenumbers (Fig. 3b), the Raman spectrum is very similar with other reported spectra for amorphous titania nanostructures [10,13,14], with three very broad peaks around 150, 450 and 600 cm^{-1} that can be attributed to Ti—O vibrations. For comparison, the Raman spectrum of the commercial Evonik-Degussa P-25 powder was superimposed in Fig. 4b. The powder is mainly crystalline anatase with traces of rutile, and it clearly exhibits all five expected anatase Raman shifts around 144, 196, 394, 516 and 638 cm^{-1} [15], with a weak peak and a weak shoulder around the expected rutile Raman shifts at 448 cm^{-1} and 613 cm^{-1} [15],respectively. This confirms that the tubes are mostly amorphous, with locally crystallized areas. For high wavenumbers (Fig. 4c), wide bands around 1600, 2100, and 3200 cm^{-1} have been observed, and they can be attributed to hydroxyl bending and stretching modes [12,16]. The role of such surface adsorbed hydroxyl groups on the antibacterial activity is explored into more detail in a later section.

The effect of obtained TiO_2-NT powders on the biological activity of *E. coli* and *S. aureus* was determined by evaluation of the growth of the cultures in the presence of photocatalysts, compared with the growth of the bacterial cultures in medium only. Data presented in Table 1 and on Fig. 5 show the results of a biological evaluation performed for test material TiO_2-NT, reference Evonik Degussa P-25 (P25) and control samples. It was observed that both P25 and control samples exhibited similar trend of growth in two different light conditions. After one hour of the experiment an initial period with a minimal bacterial growth associated with adapting to a new environment was observed (lag phase). This short, transitional period was followed by the phase of exponential growth of bacteria (log phase) for the remaining time of the experiment, with the exception of *S. aureus* cultured without the light, where the stationary phase began after 6 h. Microorganisms used in this experiment responded differently to exposure to TiO_2-NT suspensions in changing light conditions. When exposed to a UV light, both *E. coli* and *S. aureus* exhibited reduced growth and after 24 h of exposition 97.53% of *E. coli* and 99.94% of *S. aureus* were inactivated. No reduction in growth was observed after 24 h of the experiment carried out in the absence of the UV light, however the number of living microorganisms in the test group exposed to TiO_2-NT powders was significantly lower than in the group exposed to a reference material P25, and in a control group. This phenomenon suggests that antimicrobial properties exhibited by TiO_2-NT may be determined by the unique combination of the architectural, structural and chemical properties of the nanotubes. For instance, nano-tubes may physically damage cell walls, causing physical damage of the

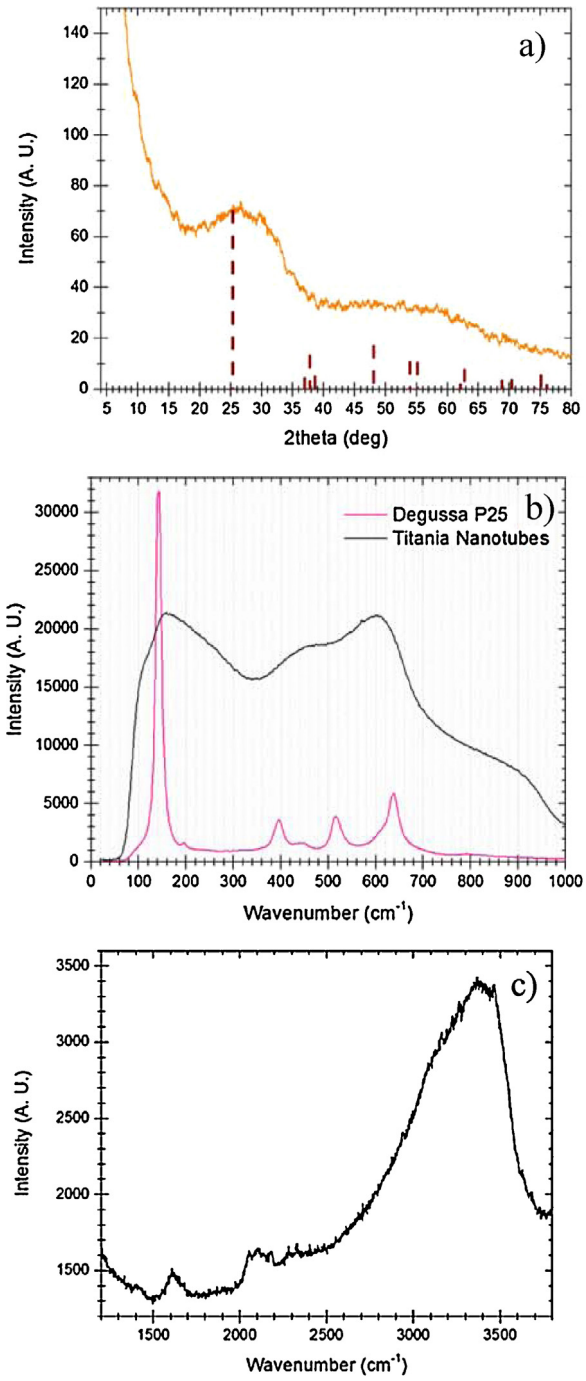

Fig. 4. (a) XRD spectrum; vertical lines represent the standard polydispersed anatase peaks, with their corresponding intensity (PDF #71-1166); (b) low wavenumbers Raman spectrum of titania nanotubes and Evonik Degussa P-25 powder; (c) High wavenumbers Raman spectrum of titania nanotubes (please note that the scale is significantly different than in the previous panel).

bacteria and their subsequent biological inactivation even when light is not available.

UV-light induced bacterial disinfection using semiconductor nanomaterials has been well demonstrated (Fig. 6) [13–19]. The initial reaction starts with the UV light-induced generation of a conduction band electron (e^-_{CB}) and a valence band hole (h^+_{VB}) [1,19]. These photo-generated electrons (e^-_{CB}) can reduce oxygen in the atmosphere to produce superoxide radicals ($^\bullet O_2^-$). Further oxidation of superoxide radicals by h^+_{VB} produces singlet oxygen ($^1O_2$). The h^+_{VB} can further react with water to produce hydroxyl radicals ($^\bullet$OH), hydrogen peroxide (H_2O_2) or protonated superoxide radical ($^\bullet HO_2$). H_2O_2 can further react with $^\bullet$OH radicals to form $^\bullet HO_2$. These reactive oxygen species (ROS) such as $^\bullet$OH, $^1O_2$, $^\bullet O_2^-$, $^\bullet HO_2$, H_2O_2, results in the decomposition of bacteria [1,20–26]. In addition, the attachment of the nanotubes to the bacterial cell membrane may upset the permeability of the cell, induces oxidative stresses and prevents the cell growth [17,18].

It is interesting to observe that despite well-known photocatalytic properties of Degussa P25 previously reported by other researchers, its antimicrobial activity was significantly compromised in our experiment [27]. A lack of an observable antimicrobial activity can be determined by a number of factors. In a study on the biological activity of the TiO_2, Yemmireddy et al. [28] reported that type, source and physicochemical properties of TiO_2, as well

Table 1
Concentrations of a bacterial suspension test for the reference and test samples presented as colony forming units (CFU)/mL. % Reduction (% Red) calculated after 24 h of experiment = 100 − ((T_{24} ×100%)/T_0), where T_0 – relative cell count at the start of experiment (CFU/mL), and T_{24} – relative cell count at the end of experiment.

	Sample/Light conditions					
	TiO_2-NT light	P25 light	Control light	TiO_2-NT dark	P25 dark	Control dark
E. coli 0 h	9.93×10^3	9.91×10^3	9.92×10^3	9.90×10^3	9.90×10^3	9.90×10^3
E. coli 1 h	6.35×10^3	7.00×10^3	9.70×10^3	4.55×10^3	6.60×10^3	1.13×10^4
E. coli 6 h	2.30×10^3	2.90×10^4	1.96×10^4	5.80×10^3	2.63×10^4	3.10×10^4
E. coli 24 h	2.45×10^2	8.63×10^5	8.46×10^5	1.01×10^4	1.55×10^6	1.15×10^6
% Red (24 h)	97.53%	0	0	0	0	0
S. aureus 0 h	9.01×10^3	9.07×10^3	9.00×10^3	9.01×10^3	9.07×10^3	9.00×10^3
S. aureus 1 h	4.80×10^3	9.60×10^3	9.83×10^3	6.20×10^3	9.72×10^3	1.10×10^4
S. aureus 6 h	2.90×10^3	1.64×10^4	7.48×10^4	4.86×10^3	1.52×10^6	9.32×10^4
S. aureus 24 h	5.00×10^0	9.04×10^5	1.06×10^6	3.42×10^4	1.55×10^6	1.16×10^6
% Red (24 h)	99.94%	0	0	0	0	0

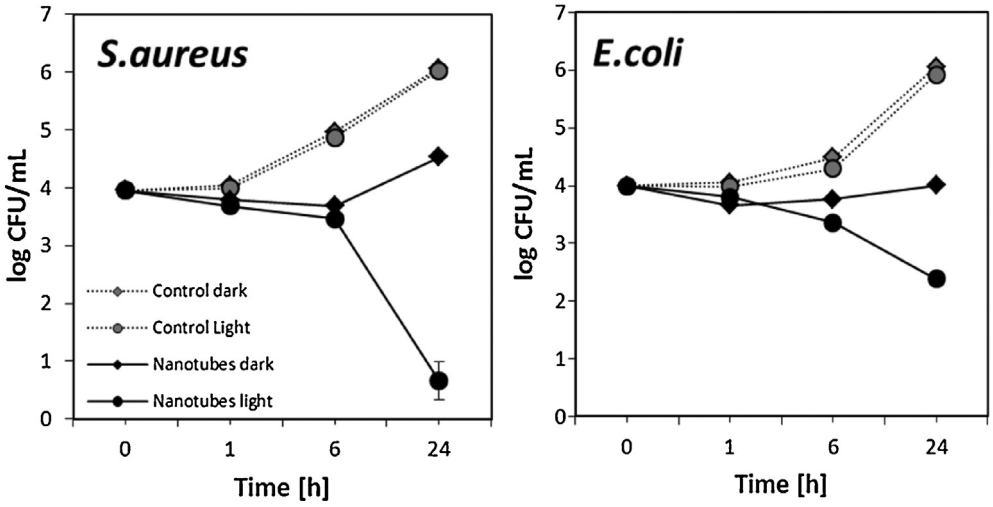

Fig. 5. The effect of obtained TiO_2-NT powders on the biological activity of bacteria. Reduction in cell viability for *E. coli* and *S. aureus*. M-H broth inoculated with bacteria only served as a positive control. Error ± SD for $n = 3$.

as experimental conditions of the biological investigations, play an important role during the bacterial inactivation. These parameters may affect the rate of the reactive oxygen species (ROS) formation, which is a function of nanostructure, specific surface area, particle size, crystalline phase or the light intensity. It is also known that UV light has very limited penetrating power; therefore any physical barrier acting as a shield around the photocatalyst may reduce the rate of the microbial inactivation. In our experiment, it was observed that Degussa P25 in M-H medium in concentration of 50 mg/mL, formed opaque suspension in comparison to the appearance exhibited by equivalent concentrations of the TiO_2-NT. This phenomenon could also contribute to reduced photocatalytic properties of the Degussa P25. In addition, the spontaneous crystallisation of amorphous anodized titania nanotubes by soaking in water at room temperature was previously reported [29]. The water present in the bacteria culture medium also might have turned some of the amorphous titania to crystalline anatase TiO_2 during the antibacterial studies. It should also be noted that the

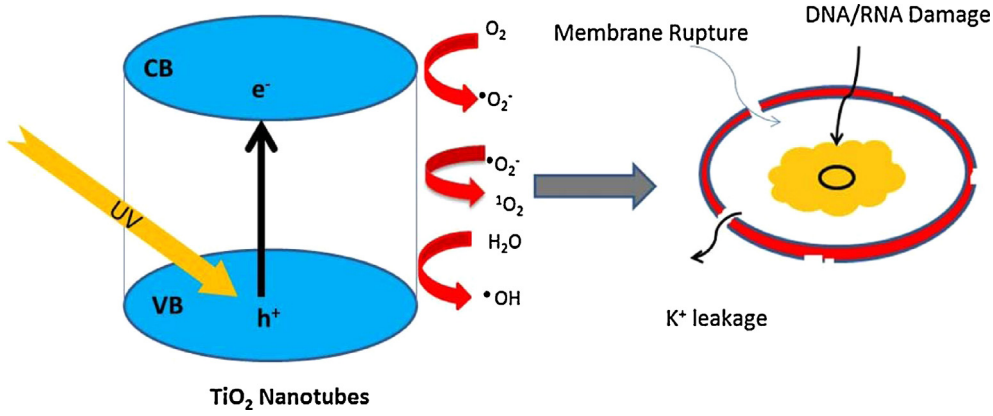

Fig. 6. Schematic representation of the photocatalytic bacterial disinfection.

adsorption of bacterial cell on the titania surfaces is highly significant in achieving anti-bacterial activity [30]. The nanotubes with a number of active hydroxyl groups could enhance the "adsorption" of bacteria and thereby increased antibacterial properties can be observed.

4. Conclusions

The anti-microbial properties of the TiO_2 nanotubes prepared by a rapid breakdown anodization process were studied and compared with Evonic-Degussa P25. TiO_2 Nanotubes showed excellent antibacterial properties against *E. coli* (97.53%) and *S. aureus* (99.94%) under 24 h of UV irradiation, while commercial and control samples did not show any antimicrobial properties. It has been noted that the morphology, surface properties and physicochemical properties of TiO_2 nanotubes, as well as experimental conditions of the biological analysis, play a significant role in the antibacterial activity.

Acknowledgement

One of the authors S.C. Pillai wishes to acknowledge financial support under the US-Ireland R&D Partnership Initiative from the Science Foundation Ireland (SFI-grant number 10/US/I1822 (T)).

References

[1] S. Banerjee, S.C. Pillai, P. Falaras, Kevin E. O'shea, J.A. Byrne, D.D. Dionysiou, J. Phys. Chem. Lett. 5 (2014) 2543–2554.
[2] S. Malato, P. Fernandez-Ibanez, M.I. Maldonado, J. Blanco, W. Gernjak, Catal. Today 147 (2009) 1–59.
[3] D.A. Keane, K.G. McGuigan, P. Fernández Ibáñez, M. Inmaculada Polo-López, J.A. Byrne, P.S.M. Dunlop, K. O'Shea, D.D. Dionysiou, S.C. Pillai, Catal. Sci. Technol. 4 (2014) 1211–1226.
[4] M.B. Fisher, D.A. Keane, P. Fernández-Ibáñez, J. Colreavy, S.J. Hinder, K.G. McGuigan, S.C. Pillai, Appl. Catal. B Environ. 130–131 (2013) 8–13.
[5] V. Etacheri, G. Michlits, M.K. Seery, S.J. Hinder, S.C. Pillai, ACS Appl. Mater. Interfaces 5 (2013) 1663–1672.
[6] D.W. Synnott, M.K. Seery, S.J. Hinder, G. Michlits, S.C. Pillai, Appl. Catal. B Environ. 130–131 (2013) 106–111.
[7] R.J. Willey, L. Menon, Adv. Mater. 19 (2007) 946–9487.
[8] C. Richter, E. Panaitescu, R.J. Willey, L. Menon, J. Mater. Res. 22 (2007) 1624–1631.
[9] E. Panaitescu, C. Richter, L. Menon, J. Electrochem. Soc. 155 (2008) 7–13.
[10] A.G. Gaynor, R.J. Gonzalez, R.M. Davis, R. Zallen, J. Mater. Res. 12 (1997) 1755–1765.
[11] N.F. Fahim, T. Sekino, Chem. Mater. 21 (2009) 1967–1969.
[12] T. Gao, H. Fjellvag, P. Norby, J. Phys. Chem. B 112 (2008) 9400–9405.
[13] J. Wang, Z. Lin, Chem. Mater. 20 (2008) 1257–1261.
[14] J. Zhao, X. Wang, R. Chen, L. Li, Solid State Commun. 134 (2005) 705–710.
[15] O. Frank, M. Zukalova, B. Laskova, J. Kürti, J. Koltai, L. Kavan, Phys. Chem. Chem. Phys. 14 (2012) 14567–14572.
[16] D.M. Carey, G.M. Korenowski, J. Chem. Phys. 108 (1998) 2669–2675.
[17] J.A. Rengifo-Herrera, C. Pulgarin, Sol. Energy 84 (2010) 37–43.
[18] J.R. Harbour, M.L. Hair, J. Phys. Chem. 83 (1979) 652–656.
[19] W.A. Jacoby, P.C. Maness, E.J. Wolfrum, D.M. Blake, J.A. Fennel, Environ. Sci. Technol. 32 (1998) 2650–2653.
[20] O. Akhavan, E. Ghaderi, Carbon 50 (2012) 1853–1860.
[21] P. Suyana, S.N. Kumar, B.S.D. Kumar, B.N. Nair, S.C. Pillai, A.P. Mohamed, K.G.K. Warrier, U.S. Hareesh, RSC Adv. 4 (2014) 8439.
[22] K.M. Razeeb, J. Podporska-Carroll, M. Jamal, M. Hasan, M. Nolan, D.E. McCormack, B. Quilty, S.B. Newcomb, S.C. Pillai, Mater. Lett. 128 (2014) 60–63.
[23] M. Pelaez, N.T. Nolan, S.C. Pillai, M.K. Seery, P. Falaras, A.G. Kontos, P.S.M. Dunlop, J.W.J. Hamilton, J.A. Byrne, K. O'Shea, M.H. Entezari, D.D. Dionysiou, Appl. Catal. B Environ. 125 (2012) 331–349.
[24] C. Zhao, M. Pelaez, D.D. Dionysiou, S.C. Pillai, J.A. Byrne, K.E. O'shea, Catal. Today 224 (2014) 70–76.
[25] O. Yamamoto, Int. J. Inorg. Mater. 3 (2001) 643.
[26] M. Fang, J.H. Chen, X.L. Xu, P.H. Yang, H.F. Hildebrand, Int. J. Antimicrob. Agents 27 (2006) 513–527.
[27] J.A. Rengifo-Herrera, C. Pulgarin, Sol. Energy. 84 (2010) 37–43.
[28] V.K. Yemmireddy, H. Yen-Con, Food Sci. Technol. 61 (2015) 1–6.
[29] D. Wang, L. Liu, F. Zhang, K. Tao, E. Pippel, K. Domen, Nano. Lett. 11 (2011) 3649–3655.
[30] A. Rengifo-Herrera, A.G. Rincón, C. Pulgarin, Photocatalysis and Water Purification: From Fundamentals to Recent Applications, in: P. Pichat (Ed.), Wiley-VCH Verlag GmbH & Co. KGaA, Weinheim, 2013, pp. 295–311.